LA-UR- 08-6854

Approved for public release; distribution is unlimited.

Title:	Estimating in vivo death rates of targets due to CD8 T cell-mediated killing
Author(s):	V. Ganusov, Z#224069, T-10/T-Division
Intended for:	Journal: Journal of Virology

Los Alamos
NATIONAL LABORATORY
EST. 1943

Form 836 (7/06)

Estimating in vivo death rates of targets due to CD8 T cell-mediated killing

Vitaly V. Ganusov*and Rob J. De Boer

Theoretical Biology, Utrecht University,

Padualaan 8, 3584 CH Utrecht, The Netherlands.

Emails: vitaly.ganusov@gmail.com, R.J.DeBoer@uu.nl

September 16, 2008

Abstract

Despite recent advances in immunology, several key parameters determining virus dynamics in infected hosts remain largely unknown. For example, the rate at which specific effector and memory CD8 T cells clear virus-infected cells in vivo, is hardly known for any viral infection. We propose a framework to quantify T cell mediated killing of infected or peptide-pulsed target cells using the widely used assay of in vivo cytotoxicity. We reanalyze recently published data on killing of peptide-pulsed splenocytes by cytotoxic T lymphocytes and memory CD8 T cells specific to NP396 and GP276 epitopes of LCMV in the mouse spleen. Because there are so many effector CD8 T cells in spleens of mice at the peak of the immune response, NP396- and GP276-pulsed targets are estimated to have very short half-lifes of 2 and 14 minutes, respectively. After the effector numbers have diminished, i.e., in LCMV-immune mice, the half-lifes become 48 minutes and 2.8 hours for NP396- and GP276-expressing targets, respectively. Analysis of several alternative models demonstrates that the estimates of half-life times of peptide-pulsed targets are robust to changes in the model assumptions. Our report provides a unifying framework to compare killing efficacy of CD8 T cell responses specific to different viral and bacterial infections in vivo, that may be used to compare efficacy of various CTL-based vaccines.

Abbreviations: LCMV, lymphocytic choriomeningitis virus, CTLs, cytotoxic T lymphocytes, TDLs, thoracic duct lymphocytes, CIs, confidence intervals, RSS, residual sum of squares.

*On the leave of absence from Institute of Biophysics and Krasnoyarsk Science Center, Siberian Branch of the Russian Academy of Sciences, Akademgorodok, Russia, 660036

1 Introduction

The time course of a CD8 T cell response to several acute viral infections in mice is well understood (3, 18, 52), but several key parameters determining dynamics of the virus and virus-specific CD8 T cells are yet to be determined. For example, the death rate of virus-infected cells due to a CD8 T cell response and the per capita killing efficacy of CD8 T cells is hardly known for most viral infections.

In a series of elegant articles, a new experimental method for measuring cytotoxicity of peptide-specific CD8 T cells in vivo was introduced (2, 7, 15, 30, 32). In this assay, peptide-pulsed and unpulsed target cells are transferred into mice harboring epitope-specific T cells, and elimination of pulsed targets is used as indication of Ag-specific killing in vivo (6, 13, 16, 28) (reviewed in (29)). Despite of the widespread use of this technique to measure epitope-specific killing in acute and chronic viral infections (1, 23, 25, 33, 40, 42, 44, 49), by naive CD8 T cells (14), by CD4+ T cells (11), or during graft rejection (21), the output of the assay remains semi-quantitative. Usually, one reports the percent killing of peptide-pulsed targets in a short term killing assay. Due to semi-quantitative nature of the assay, it is hard to compare the efficacy of CD8 T cell responses to different agents in vivo, e.g., due to different time windows used for the assay, different tissues sampled (e.g., spleen, lung, lymph nodes), different numbers of CD8 T cells present in the tissue, etc. In contrast, killing of target cells in vitro has been investigated in great detail (34–36).

In this report we illustrate how the killing efficacy of CD8 T cell responses can be estimated using the in vivo cytotoxicity assay. Currently, there are two types of experiments in which CD8 T cell mediated cytotoxicity is measured in vivo. In a few studies, killing of peptide-pulsed targets is recorded in a time series regularly over a short time period (6, 13), but in most other experiments killing is measured at a single time point. In this report we demonstrate how using either time series data or single point measurements, one can estimate the death rate or half-life times of peptide-pulsed targets due to CD8 T cell mediated killing.

Our work builds upon several previous studies attempted to estimate killing efficacy of CD8 T cells in vivo, and adds several improvements to the previous analysis (7, 37, 51). In a pioneering study, Barchet *et al.* (7) have estimated the half-life of target cells, expressing the GP33 epitope of LCMV, at the peak of the immune response to LCMV. As we show here their study underestimated the killing efficacy of the GP33-specific CD8 T cell response, by assuming rapid migration of target cells from the blood to the spleen. Regoes *et al.* (37) extended the previous study by explicitly describing recruitment of targets from the blood to the spleen, and by estimating the per capita killing efficacy of memory and effector CD8 T cells specific to two epitopes of LCMV. Yates *et al.* (51) further extended this work by proposing a different fitting procedure for the estimation of the per capita killing efficacy of CD8 T cells. In this paper we

show that the model, originally proposed by Regoes *et al.* (37), does not adequately describe the loss of peptide-pulsed targets over time in the data of Barber *et al.* (6). We formulate several alternative models that are more consistent with the analyzed data, and show that from a single measurement of in vivo cytotoxicity one can estimate the death rate of target cells due to CD8 T cell-mediated killing. Finally, we demonstrate that the estimates of the death rate of pulsed targets are robust to several changes in the model. In contrast, the estimates of the per capita killing efficacy of CD8 T cells in vivo depend critically on the model assumptions (Ganusov and De Boer, ms. in preparation), and therefore are less reliable. These results strongly argue that in the absence of a better understanding of the process of killing of cells in the spleen, one should aim at estimating the overall efficacy of CD8 T cell responses by calculating the death rate or half-life times of peptide-pulsed targets and not by estimating the per capita killing efficacy of CTLs as has been done before (37, 51). We also suggest additional experiments for further testing of specific predictions of the analyzed models that may allow for better understanding of how viral infections are controlled by CD8 T cell responses.

2 Material and Methods

2.1 Cytotoxicity in vivo

The method of measuring cytotoxicity of CD8 T cells in vivo has been described in detail elsewhere (29). In short, a population of mouse splenocytes is labeled with an intermediate concentration of CFSE and incubated with a relevant peptide in vitro (pulsed targets). Another population of splenocytes is labeled with a high concentration of CFSE and left unpulsed (unpulsed targets). Both peptide-pulsed and unpulsed cell populations are transferred into syngenic hosts (generally i.v.), and the loss of peptide-pulsed targets is measured in the organ of interest, usually the mouse spleen. The percent killing is estimated from the reduction in the ratio of the percentage of pulsed target cells to unpulsed cells, which is corrected for the initial ratio (29). This calculation is similar to that used in the standard ^{51}Cr release assay (6). For example, if 4 hours after cell transfer, 10% of pulsed and 90% of unpulsed cells are recovered from the mouse spleen ($R_1 = 0.10/0.90$), and the initial ratio of pulsed to unpulsed cells was 45% to 55% ($R_2 = 0.45/0.55$), then the (corrected) ratio of pulsed to unpulsed targets is $R = R_1/R_2 = 0.10/0.90 : 0.45/0.55 \approx 0.14$ and the percent killing is $L = 1 - R = 86\%$ (29).

In this report, we analyze recently published data on killing of peptide-pulsed splenocytes by LCMV-specific effector and memory CD8 T cells (6, 37). The cytotoxicity in vivo assay was conducted as described above with some modifications. Target splenocytes were pulsed with NP396 or GP276 peptides of LCMV, or were left unpulsed. Cells were transferred into syngenic mice either infected with LCMV 8 days before ("acutely infected" mice), or into mice recovered

from LCMV infection (LCMV-immune or "memory" mice). At day 8 after the infection, the CD8 T cell response to LCMV reaches its peak, and by 30 to 40 days after the infection, the CD8 T cell response contracts and the memory phase starts (3, 31). At different times after the transfer of target cells, spleens were harvested, and the number of pulsed and unpulsed targets, splenocytes, and peptide-specific CD8 T cells was measured.

2.2 Mathematical model for the cytotoxicity in vivo assay

Following intravenous (i.v.) injection, target splenocytes migrate to different tissues. The route of recirculation of splenocytes in mice has not been thoroughly investigated, however. Migration of radioactively labeled lymphocytes, mainly thoracic duct lymphocytes, from the blood to different organs and back to blood has been extensively studied in rats and sheep (22, 38, 39, 45, 47), but may be different from that of splenocytes (38, 39). From previous studies it is expected that many splenocytes enter the spleen (22, 39), one of the major lymphoid organs (24). Given these immunological details, modeling migration of pulsed and unpulsed targets from the blood to the spleen (or potentially other organ of interest) is done with a two compartment model similar to the one that has been proposed earlier (37).

Target cells injected i.v. migrate from the blood to the spleen at a rate σ, die at a rate ϵ due to preparation techniques (independent of CD8 T cell mediated killing), or migrate to other tissues and/or die elsewhere at a rate δ. Because of the method of obtaining single cell suspensions (e.g., mincing the spleen or pushing it through a mesh) and long handling times, transferred splenocytes are expected to have some intrinsic death rate (27). Additional indirect evidence of low survival of splenocytes comes from the observation that generally only 10% or less of adoptively transferred lymphocytes (or splenocytes) are recovered in the spleen and major lymph nodes of recipient mice (26, 50). This is in contrast with thoracic duct lymphocytes, sampled from the lymph and therefore expected to undergo less mechanical death, since up to 80 to 90% of TDLs are recovered after adoptive transfer in rats (39, 46, 47). In the spleen, unpulsed and pulsed targets die due to preparation-induced death rate ϵ, and pulsed targets also die due to CD8 T cell mediated killing, described by the rate K. The model equations are

$$\frac{\mathrm{d}S_B(t)}{\mathrm{d}t} = -(\delta+\sigma+\epsilon)S_B(t), \tag{1}$$

$$\frac{\mathrm{d}S(t)}{\mathrm{d}t} = \sigma S_B(t) - \epsilon S(t), \tag{2}$$

$$\frac{\mathrm{d}T_B(t)}{\mathrm{d}t} = -(\delta+\sigma+\epsilon)T_B(t), \tag{3}$$

$$\frac{\mathrm{d}T(t)}{\mathrm{d}t} = \sigma T_B(t) - \epsilon T(t) - KT(t), \tag{4}$$

where $S_B(t)$ and $T_B(t)$ are the numbers of unpulsed and peptide-pulsed target cells in the blood, respectively, and $S(t)$ and $T(t)$ is the number of unpulsed and pulsed targets in the spleen, respectively, σ is the rate of migration of target cells from the blood into the spleen, and δ is the rate of cell migration/death from blood to other organs, ϵ is the extra death rate of transferred splenocytes due to preparation (independent of epitope-specific CD8 T cells), and K is the death rate of peptide-pulsed targets due to CD8 T cell mediated killing in the spleen. The initial conditions for the model are $S_B(0) = T_B(0) = 5 \times 10^6$ cells and $S(0) = T(0) = 0$ (6). Because there is a constant number of epitope-specific CD8 T cells in the spleen in 4 hour experiments (data not shown), the death rate of peptide-pulsed targets K due to CD8 T cell mediated killing is assumed to be constant over time. Note that in this formulation of the model, we assume that there is no specific killing of peptide-pulsed targets in the blood (see Alternative models). Also note that we extend the previously suggested model (37) by adding an extra death rate ϵ due to preparation of targets. As we show in the main text, this extension is absolutely required for a satisfactory description of the data. One can easily solve the model equations and arrive at following formulas

$$S(t) = \frac{c}{d-\epsilon}\left[\mathrm{e}^{-\epsilon t} - \mathrm{e}^{-dt}\right], \tag{5}$$

$$R(t) = \frac{(d-\epsilon)}{(\epsilon+K-d)}\left[\frac{\mathrm{e}^{-dt} - \mathrm{e}^{-(\epsilon+K)t}}{\mathrm{e}^{-\epsilon t} - \mathrm{e}^{-dt}}\right], \tag{6}$$

where $d = \sigma + \epsilon + \delta$ is the rate of removal of cells from the blood, $c = S_B(0)\sigma$, and $R(t) = T(t)/S(t)$ is the ratio of the number of pulsed to unpulsed targets in the spleen at time t. A simple analysis shows that the decline in the logarithm of the ratio, $\log(R(t))$ over time is biphasic with the initial decline rate $K/2$, and a slower rate thereafter being determined by the difference between the rate of removal of targets from the blood d and the preparation-induced death rate ϵ (if $K > d$, see Figure 2 and Appendix). Fitting simple exponential or bi-exponential functions to data on the decline in the ratio $R(t)$ for NP396- and GP276-pulsed targets in acutely infected mice confirms the biphasic nature of the decline (single vs. double exponential decline fitted to $\arcsin(\sqrt{R})$ transformed data, $F_{2,34} = 70.45$, $p \ll 0.001$ for NP396-pulsed targets, and $F_{2,34} = 10.27$, $p \ll 0.01$ for GP276-pulsed targets). The $\arcsin(\sqrt{R})$ transformation is widely used to normalize frequency data distributed between 0 and 1 (53).

When killing of peptide-pulsed targets is measured at several time points after the transfer, one should fit the model solutions given in eqn. (5) and (6) to the data to estimate the death rate of peptide-pulsed targets K due to CD8 T cell mediated killing.

When the killing assay is done for one time point, one can obtain an estimate of the minimal and maximal death rate of peptide-pulsed targets K under the assumptions of the above model and assuming small preparation-induced cell death rate (i.e., $\epsilon \to 0$; see Supplementary Infor-

mation). The upper bound estimate for K is obtained by assuming that the rate of removal of cells from the blood is minimal, i.e., $d \to 0$. The estimate of the death rate of peptide-pulsed targets $K_{\max}$ is then found by solving the transcendental equation:

$$K_{\max} = \frac{1 - e^{-K_{\max} t}}{Rt}, \tag{7}$$

where R is the ratio of pulsed to unpulsed targets at time of the assay t. Note that when the death rate $K_{\max}$ is large (i.e., $K_{\max} t \gg 1$), then $K_{\max} \approx 1/(Rt)$. The minimal estimate for the death rate of infected cells, $K_{\min}$, is found when migration of target cells into the organ where the killing occurs is instantaneous (i.e., when $\sigma \to \infty$ in eqn. (6)):

$$K_{\min} = -\frac{\ln R}{t}. \tag{8}$$

Survival of peptide-pulsed targets can also be expressed as half-lifes, $T_{1/2} = \ln 2/K$, $T_{\min} = \ln 2/K_{\max}$ and $T_{\max} = \ln 2/K_{\min}$. Note that to determine the death rate of targets due to CD8 T cell mediated killing one needs not measure the number of epitope-specific CD8 T cells at the site of killing.

It should be noted, however, that besides the main model with the preparation-induced cell death (given in eqn. (5)–(6)), several alternative models can describe the data on killing of peptide-pulsed targets with reasonable quality. However, as we discuss in the Results section, these models require specific parameter values that we believe are not consistent with available data. Nevertheless, additional experemental data are required to discriminate between the alternative models.

2.3 Estimation of the death rate of target cells from the time series data

We fit the data on recruitment of unpulsed cells into the spleen ("recruitment" data) and on killing of peptide-pulsed target cells ("killing" data) with the model simultaneously for all 6 populations of cells (i.e., unpulsed and pulsed with either the NP396 or GP276 epitope) in acutely infected or memory mice using eqn. (5) and (6).

To describe recruitment of target cells from the blood to the spleen, we assume that the recruitment occurs at different rates in different mice. Indeed, plotting the total number of unpulsed target cells in the spleen versus the number of splenocytes for any particular time point, reveals that the number of target cells, recruited into the spleen, increases with the spleen size (Figure 1). Therefore, for every mouse, the rate of entrance of cells into the spleen, σ, is assumed to depend linearly on the number of splenocytes,

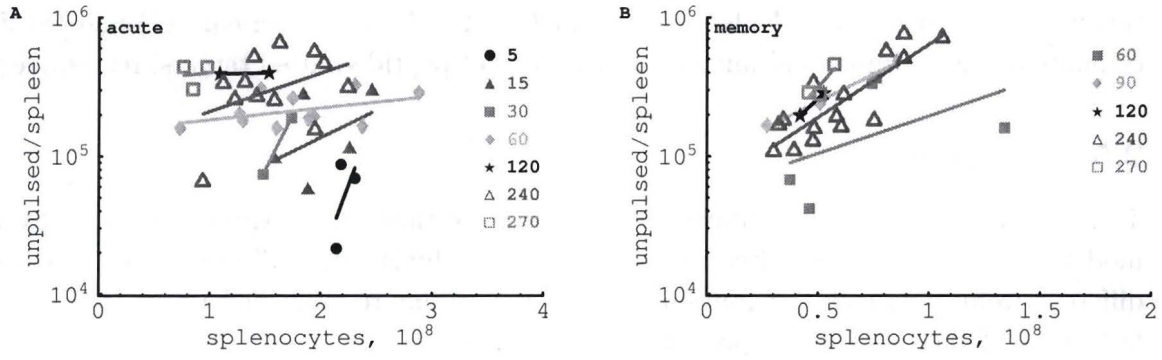

Figure 1: Plotting correlations between the number of unpulsed cells found in the spleen at different time points after transfer (shown in minutes) as the function of the number of splenocytes in acutely infected (panel A) and memory (panel B) mice. There is a positive correlation between the total number of unpulsed cells found and the number of splenocytes for most time points analyzed. This suggests that the rate of recruitment of targets into the spleen depends on the spleen size.

$$\sigma_i = \alpha \times (N_s)_i \tag{9}$$

where $(N_s)_i$ is the number of splenocytes in the i^{th} mouse and α is a coefficient. Because there are more splenocytes in acutely infected mice than in spleens of memory mice, we allow for two coefficients α_A and α_M to relate the rate of recruitment of targets from blood to the spleen and spleen size in acutely infected and memory mice, respectively. The extra death rate of targets ϵ and the rate of migration to other organs δ are assumed to be the same in different mice.

Targets pulsed with different peptides may have different death rates in the spleen due to CD8 T cell-mediated killing, in part due to different sizes of populations of epitope-specific CD8 T cells. Then K^a_{NP} and K^a_{GP} are the death rates of NP396- and GP276-expressing targets in acutely infected mice (due to killing by effector CD8 T cells). Similarly, K^m_{NP} and K^m_{GP} are the death rates of NP396- and GP276-expressing targets in memory mice (due to killing by memory CD8 T cells).

2.4 Estimation of the death rates of target cells from a single time point

Measuring killing of peptide-pulsed targets at one time point does not allow for a rigorous test of different modeling approaches (as shown in Results). However, using the simple formulas given in eqn. (7) and (8), one can obtain maximal and minimal estimates of the death rate of peptide-pulsed targets due to CD8 T cell mediated killing. Specifically, for every measured fraction of

target cells killed L, one calculates the ratio $R = 1 - L$, and using eqn. (7) and (8) finds an estimate of the maximal and minimal death rates of peptide-pulsed targets, respectively.

2.5 Statistics

To fit both recruitment and killing data at the same time we log-transform the data and the model predictions. This resulted in well-behaved residuals with a distribution statistically not different from a normal distribution (8, $p = 0.08$, Shapiro-Wilk normality test). To access lack of fit of the data with repeated measures we use the F-test (8, p. 29). To compare the quality of the fit of different models, we perform the partial F test to compare two nested models by the difference between their residual sum of squares (RSS) per additional parameter divided by the residual mean square of the largest of the two models (8, p.104). The residual mean square (MNSQ) is RSS divided by the residual degrees of freedom, i.e., the difference between the number of data points and the number of free parameters (8). The F distribution is parameterized by 2 degrees of freedom, $F_{n,k}$. The one in the numerator (n) is the difference in the number of parameters between the two models. The one in the denominator (k) is the number of degrees of freedom of the largest model (i.e., the number of data points minus the number of parameters). Fittings were done in Mathematica 5.2 using the FindMinimum routine.

3 Results

3.1 Estimating the death rate of peptide-pulsed targets using time series data

We propose a mathematical model to estimate the killing efficacy of CD8 T cell responses using the in vivo cytotoxicity assay. The model describes the recruitment of unpulsed targets from the blood to the spleen, and the decline of the ratio of peptide-pulsed to unpulsed targets over time due to CD8 T cell mediated killing. Two mechanisms are included in the model: 1) target cells may die because of the preparation of single cell suspensions, and 2) the rate of recruitment of targets cells from the blood to the spleen depends on the spleen size in individual mice. The model was fitted to the data on killing of NP396- and GP276-pulsed targets in mice, acutely infected with LCMV (8 days after the infection), and LCMV-immune, memory mice (see Material and Methods for more detail).

We find that the proposed model (given in eqn. (5)–(6)) describes reasonably well the recruitment of unpulsed targets into the spleens of acutely infected and LCMV-immune mice (Figure 2A&B). This result suggests that the rate of recruitment of cells into the spleen was

dependent on the spleen size (see also Figure 1). This was also true for acutely infected mice since assuming a constant rate of cell recruitment into the spleen in acutely infected mice resulted in a 25% decrease in the quality of the model fit to the data (or consequently, increase in the residual sum of squares from 14.2 to 18.9 for the data from acutely infected mice; results not shown).

Importantly, the model also predicts a biphasic decline in the ratio of NP396-pulsed to unpulsed targets over time in acutely infected mice similarly to what is observed in the data (Figure 2C); changes in the ratio are well reproduced for memory mice as well (Figure 2D&F). Overall, the data are described by the model with reasonable quality as judged by the lack of fit test ($F_{29,162} = 1.53$, $p = 0.053$; the low p-value is due to several outliers such as those shown in Figure 2C at 120 min) and by the distribution of the residuals ($p = 0.08$, Shapiro-Wilk normality test).

Interestingly, we could set the rate of migration of target cells from the blood to other organs δ to 0 without reducing the quality of the model fit to data ($F_{1,190} = 0.17$, $p = 0.68$). This suggests little or no migration of cells to other organs of mice. Reducing the number of other parameters in the model always resulted in a significantly worse description of the data. In particular, setting the rate of the preparation-induced cell death rate ϵ to 0 (in the model where $\delta > 0$) resulted in significantly worse fits of the data ($F_{1,190} = 19.82$, $p \ll 0.001$), mainly because of a poor description of recruitment of unpulsed targets into the spleen. This argues that the previously suggested model (37), which lacked this extra parameter, does not provide a satisfactory description of the data. This is further confirmed by the lack of fit test of the model with $\epsilon = 0$ ($F_{29,162} = 2.26$, $p \ll 0.01$). Allowing for $\alpha_A = \alpha_M$ (these parameters determine the rate of cell migration from the blood to the spleen in acutely infected and memory mice, respectively) also resulted in significantly worse fits of the data ($F_{1,191} = 13.59$, $p < 0.001$).

Finally, assuming that recruitment of target cells from the blood to the spleen occurs similarly in all mice, i.e., independently of their spleen size, led to much worse fits of the data (RSS=72.57). This further argues in favor of our hypothesis that recruitment of target cells into the spleen occurs at different rates in different mice.

Our analysis provides novel estimates for the half-life times (or death rates) of peptide-pulsed target cells in spleens of mice acutely infected and in mice that have cleared LCMV. We find that NP396- and GP276-pulsed targets have a half-life of 2 and 14 minutes in acutely infected mice, while half of pulsed targets are eliminated in 48 minutes and 2.8 hours in memory mice. The short half-life of peptide-pulsed targets in acutely infected mice is most likely due to a large population of epitope-specific CD8 T cells, present at the peak of the immune response.

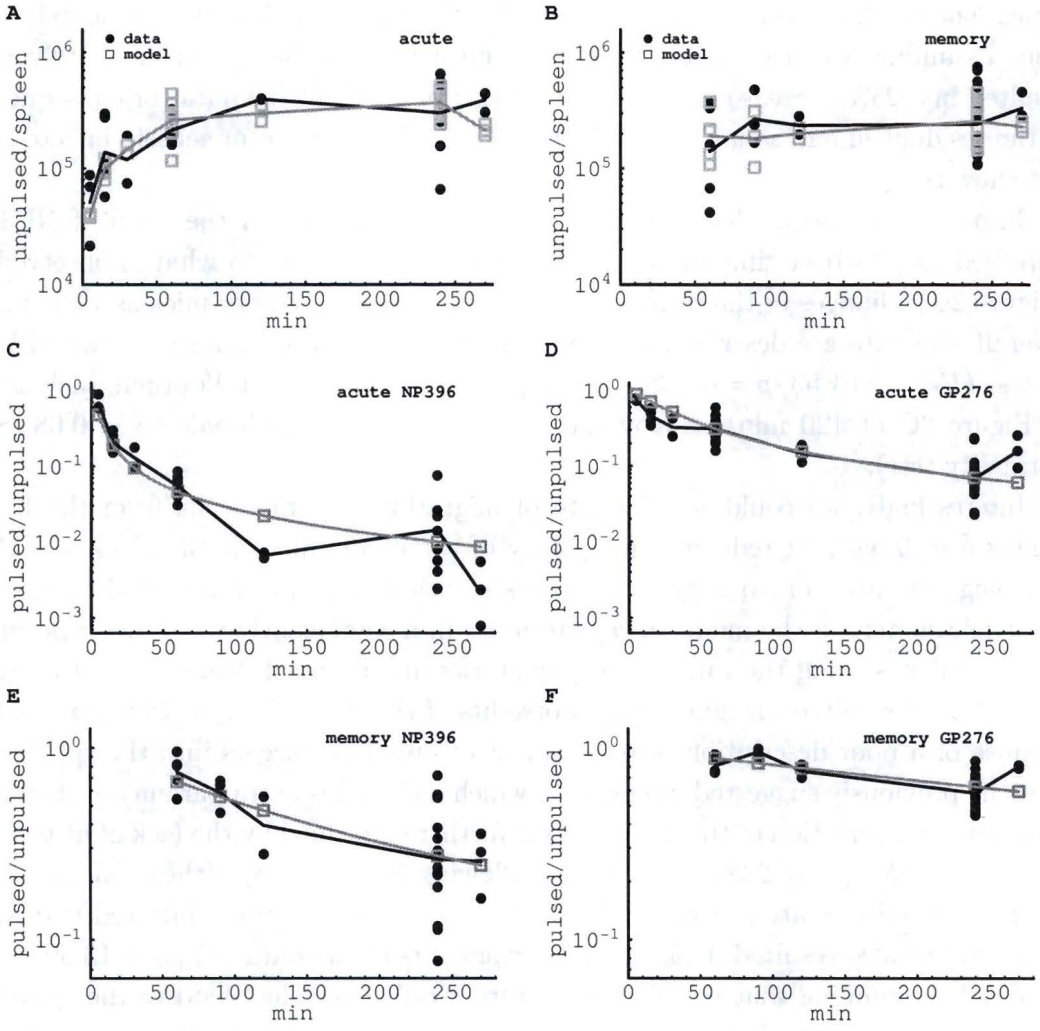

Figure 2: Fitting the data on recruitment of target cells to the spleen (A-B) and on killing of peptide-pulsed targets in the spleen (C-F). Panels A and B show the recruitment of unpulsed targets into the spleen, and panels C-F show the decline in the the ratio of pulsed to unpulsed targets in the spleen due to CD8 T cell-mediated killing over time. Panels A, C, and D are for acutely infected mice, and panels B, E, and F are for memory mice. Panels C and E are for NP396-pulsed targets and panels D and F are for GP276-pulsed targets. Black dots (•) denote measurements from individual mice, and black lines denote the log average value per time point. Gray boxes (□) show the number of recruited cells predicted by the model for individual mice (panels A and B) or the predicted average ratio (panels C-F). Gray lines show the log average between individually predicted values (A-B) or the predicted average ratio (C-F). Note a different scale for killing of target cells in acutely infected (panels C and D) and memory (panels E and F) mice. Parameters providing the best fit of the model are shown in Table 1. The residual sum of squares (RSS) for this fit is 65.55.

Parameter	Mean	Low 95% CI	High 95% CI
ϵ, min^{-1}	4.71×10^{-3}	3.34×10^{-3}	6.17×10^{-3}
α_A, min^{-1}	7.17×10^{-12}	5.58×10^{-12}	9.22×10^{-12}
α_M, min^{-1}	1.30×10^{-11}	0.92×10^{-11}	1.89×10^{-11}
K^a_{NP}, min^{-1}	3.45×10^{-1}	2.59×10^{-1}	4.56×10^{-1}
K^a_{GP}, min^{-1}	5.0×10^{-2}	3.80×10^{-2}	6.41×10^{-2}
K^m_{NP}, min^{-1}	1.44×10^{-2}	1.10×10^{-2}	1.82×10^{-2}
K^m_{GP}, min^{-1}	4.15×10^{-3}	3.21×10^{-3}	5.52×10^{-3}

Table 1: Parameters providing the best fit of the model with preparation-induced death of targets (given in eqn. (5)–(6)) to the data. Here α_A and α_M are coefficients relating the recruitment rate of cells into the spleen in acutely infected, $\sigma = \alpha_A N_s$ and LCMV-immune mice, $\sigma = \alpha_M N_s$, and the number of splenocytes in individual mice N_s. In the fits, the rate of migration of labeled splenocytes to other organs δ was fixed to 0 since this did not affect the quality of the model fit to data ($F_{1,190} = 0.15$, $p = 0.68$). Data and model fits are shown in Figure 2. The death rate of targets estimated by the model in acutely infected mice is $K^a_{NP} = 497$ and $K^a_{GP} = 72$ per day for NP396 and GP276-pulsed targets, respectively. In memory mice, the death rate of peptide-pulsed targets is $K^m_{NP} = 21$ and $K^m_{GP} = 6$ per day for NP396 and GP276-pulsed targets, respectively. These rates correspond to the half-lifes of 2 and 14 minutes for NP396- and GP276-expressing targets at the peak of the CD8 T cell response, and 48 minutes and 2.8 hours for NP396- and GP276-expressing targets in LCMV-immune mice, respectively. Confidence intervals (CIs) were calculated by bootstrapping the data with 1000 simulations (19).

3.2 Estimating the death rate of peptide-pulsed targets from single measurements

For every measured ratio of pulsed to unpulsed targets in the same data, we can also use the formulas given in eqn. (7) and (8) to estimate the maximal and minimal death rates of peptide pulsed targets in spleens of acutely infected or memory mice, due to CD8 T cell-mediated killing (Figure 3). The analysis shows that there is a large variability in the estimated death rates, especially for NP396-pulsed targets, suggesting a large measurement noise in estimating the percent of peptide-pulsed targets killed. Interestingly, the average of the maximum death rate of peptide-pulsed targets is only slightly higher than the predicted death rate K obtained by the analysis of the time series data (see Table 1). This argues that this method of calculation does deliver reliable estimates for the death rate of peptide-pulsed targets but may require repeated measurements of killing. In contrast, the minimal estimates of the death rates of peptide-pulsed targets are up to 10 times lower than the fitted values, especially for cases when killing is very fast (Figure 3). This discrepancy may explain the very low estimates of the death rate of peptide-pulsed targets found in a previous study (7) that assumed rapid migration of target cells from the blood to the spleen (and, therefore, estimated $K_{\min}$, see also Discussion). Since the maximum estimate of the death rate of peptide-pulsed targets is relatively robust to changing the model in various ways (for example, assuming killing of peptide-pulsed targets in the blood, see Appendix), one can use $K_{\max}$ as an upper bound estimate for the efficacy of antigen-specific CD8 T cell responses in vivo.

3.3 Alternative models, potential problems and future experimental tests

The biphasic decline in the ratio of peptide-pulsed to unpulsed targets (e.g., Figure 2C) is one of the important features of the these data that was missed in the previous analyses. There are several alternative models that can provide the slowdown of the decline in the ratio over time.

In the main model, in which target cells have a preparation induced poor survival in recipient hosts, the slowing down of the decline in the ratio R is due to a slow removal of target cells from the blood (given by the parameter $d = \epsilon + \delta + \sigma$). At very high rates of killing of peptide-pulsed targets, killing in the spleen can indeed become limited by the rate of recruitment of pulsed targets from the blood to the spleen. The preparation-induced cell death rate is then required to properly describe the recruitment of unpulsed targets from the blood to the spleen. For acutely infected mice we estimate the average rate of removal of cells from the blood $d \approx 0.006\ min^{-1}$ corresponding to the half-life of cells in the blood of 1.95 hours. To our knowledge, the rate of removal of splenocytes from circulation has not yet been estimated, and future experiments would be needed to test this quantitative prediction of our model. Interestingly, some studies

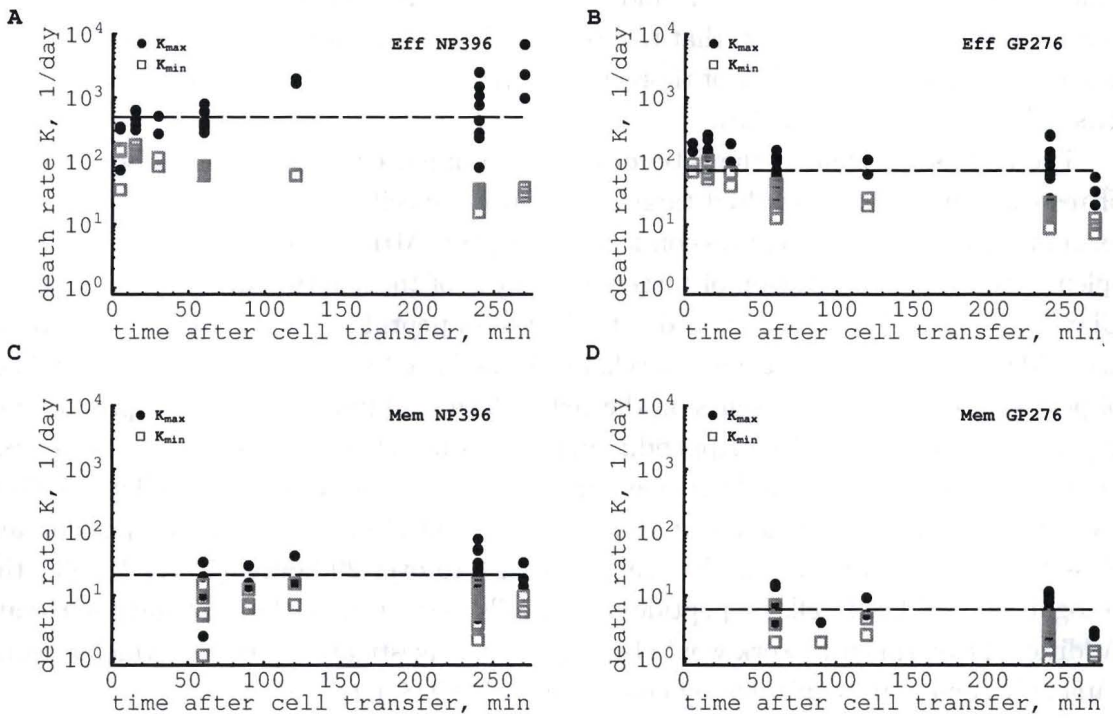

Figure 3: Maximal (•) and minimal (□) estimates of the death rate of peptide-pulsed cells, due to CD8 T cell-mediated killing, obtained from a single measurement of killing of peptide pulsed targets (using eqn. (7) and eqn. (8)). Average maximum estimates and standard deviations are: 812 ± 1160 per day (NP396 acute, panel A), 110 ± 68 per day (GP276 acute, panel B), 23 ± 17 per day (NP396 memory, panel C), 7 ± 4 per day (GP276 memory, panel D). The average minimal estimates and the standard deviations are: 68 ± 47 per day (NP396 acute), 35 ± 27 per day (GP276 acute), 8 ± 4 per day (NP396 acute), 3 ± 2 per day (GP276 memory). Dashed horizontal lines denote estimates of the death rate of peptide-pulsed targets obtained by fitting the time series data (see Figure 2 and Table 1). Large variation in individual estimates of the death rate of targets suggests that one should aim for performing longitudinal killing assays that allow for more precise estimation of the death rates of peptide-pulsed targets.

have found that transferred splenocytes can be detected in the blood for long periods of time, although the rate of their removal from the blood has not been estimated (1, 2). The net slow removal of targets from the blood could also come from influx of cells that first migrated to other organs such as lung or liver, and then back to the circulation (39, results not shown). It is important to note, however, that the estimated rate of removal of splenocytes from the blood is several fold lower than that of thoracic duct lymphocytes (TDLs) that reside in the blood of rats only for ~ 30 min (22, 39).

The biphasic decline of the ratio of pulsed to unpulsed targets could also be due to a loss of recognition of peptide-pulsed targets by epitope-specific CD8 T cells. This may occur, for example, due to different expression levels of peptide-MHC complexes on the surface of target splenocytes, due to migration of targets into areas of the spleen hardly reachable by activated CD8 T cells (e.g., B cell zones), or due to the loss of peptides from the surface of peptide-pulsed cells (51). Since the latter is most mechanistic, we have formulated a model describing the loss of peptides from MHC molecules on the cell surface, and indeed this model produced expected biphasic fits of the data (see Appendix and results not shown). The model fits suggested that peptide-pulsed targets should become unrecognizable by epitope-specific CD8 T cells with the half-life time of about 4 hours. Given that the half-life of most specific peptide and MHC class I molecule complexes in vitro ranges from 6 to over 20 hours, (5, 12, 41, 43), the loss of recognition by CD8 T cells by peptide-pulsed cells in the time scale of 4 hours seems rather fast. Additional experimental work would be required to investigate the rate at which peptide-pulsed targets become unrecognizable by epitope-specific CD8 T cells in vivo.

Our main model allowing for the preparation-induced (CD8 T cell independent) cell death predicts that at the constant death rate $\epsilon \approx 0.005\ min^{-1}$, very few unlabeled splenocytes ($\approx 0.03\%$ of the transferred number) are expected to be found in the spleen at 24 hours after the transfer. This is not realistic since it is known that at 24 hours after adoptive transfer about 5-10% of transferred cells are found in the spleen (9, 26). It is natural to assume, however, that the preparation induced death rate declines over time. This would imply that many cells die initially and fewer cells die later after preparation (27). Simple extension of the main model to include a decline in the death rate ϵ with time, i.e., $\epsilon = \epsilon_0 \times \exp[-\beta t]$, also describes the data with reasonable quality and predicts accumulation of 9% of injected unpulsed targets in the spleen by 24 hours ($\epsilon_0 = 0.013\ min^{-1}$, $\beta = 0.008\ min^{-1}$). Because the estimated rate of decline β is relatively small, this modification of the model does not affect substantially the dynamics of peptide-pulsed or unpulsed targets on the short time scale of the experiment ($F_{1,190} = 1.83$, $p = 0.18$).

Because of a relatively high estimate for the preparation-induced cell death rate, our model fits also predict a very slow rate of migration of targets to other organs, $\delta \approx 6.3 \times 10^{-4}\ min^{-1}$ (with the 95% CIs $(0, 3.5 \times 10^{-3}\ min^{-1})$). Simple analysis suggests that about 2.1×10^5 (or

maximally 1.4×10^6) injected unpulsed targets will migrate to other organs in 4 hours of the assay. Measuring the number of unpulsed targets in other organs of mice (e.g., lung or liver) at different times after cell transfer, may allow for experimental testing of this specific model prediction.

We have also formulated and analyzed another model in which cells that have migrated to the spleen can also migrate back to the blood. Kinetically, this model is very similar to the model with preparation-induced cell death (results not shown). The model also provided reasonable description of the data, and the biphasic decline in the ratio of pulsed to unpulsed targets in this model is also due to a slow removal of targets from the blood. The model also predicts a 10-fold higher rate of migration of targets to other organs of mice, $\delta \approx 5.0 \times 10^{-3}\ min^{-1}$, and as a consequence, a higher maximal number of target cells migrating to other organs ($\sim 3.1 \times 10^6$). This alternative model also estimated a relatively short half-life time of unpulsed targets in the spleen, $T_{1/2} \approx 2\ h$, which is 2 to 3 fold smaller than the estimated half-life time of thoracic duct lymphocytes in the spleen in rats (22, 39).

The biphasic decline in the ratio of peptide-pulsed to unpulsed targets could also arise if the death rate of peptide-pulsed targets due to CD8 T cell mediated killing declines over time. For example, the killing efficacy of CD8 T cells may depend on the density of peptide-pulsed targets with higher target cell densities leading to a higher killing efficacy. This, in turn, may arise if peptide-pulsed target cells stimulate CD8 T cells to increase their cytotoxicity (e.g., upregulate FasL, perforin, etc). Phenomenologically, changes in the death rate of pulsed targets with their density could be modeled by replacing the death term KT in eqn. (4) with KT^a with $a > 1$. This phenomenological model, when fitted to data, indeed allowed for the biphasic decline of the ratio R (with estimated $a = 1.68$), although the quality of the model fit to data was worse than the mechanistic models discussed above (RSS=70.55, results not shown). Thus, a poor fit of the model with density-dependent death rate of peptide-pulsed targets makes this phenomenological model less likely than a more mechanistic model with preparation-induced cell death.

In our analysis we assumed that killing of peptide-pulsed targets occurred only in the spleen. Extending the model to allow for killing of peptide-pulsed targets in the blood did not lead to a significantly better description of the data ($F_{1,191} = 0.01$, $p = 0.99$). However, future experiments may need to investigate whether any killing of peptide-pulsed targets occurs in the blood since in general this can affect estimation of model parameters (see Appendix and results not shown).

In summary, we find several realistic alternative models that describe the data well. For finer discrimination between rival models, additional experiments are necessary to test specific predictions of these models. Most importantly, the estimates of the death rates of peptide-pulsed targets due to CD8 T cell mediated killing are quantitatively similar in all these alternative

models (with the exception of the model with density-dependent death rate of targets; results not shown). This further highlights the robustness of the proposed modeling framework for estimation of the killing efficacy of CD8 T cell responses in vivo.

4 Discussion

In this report we have formulated a novel approach allowing estimation of the death rate of peptide-pulsed targets due to CD8 T cell-mediated killing from the in vivo cytotoxicity assay. We have shown how measuring killing of peptide-pulsed targets at one or several time points allows one to estimate the death rate of epitope-expressing target cells. This report, thus, forms a basis for quantification of the widely used approach to measure cytotoxicity of T cells in vivo.

A previous study using measurements of frequency of CD8 T cells in the mouse spleen following acute LCMV infection, has investigated whether effector and memory CD8 T cells have similar per capita killing efficacies (37). Here we show that in the absence of measured CTL frequencies one can estimate the death rates of peptide-pulsed targets due to CTLs and therefore measure cytotoxic efficacy of the CD8 T cell response in vivo. Neglecting the numbers of epitope-specific CD8 T cells may seem like a step backwards from previous studies (37, 51). However, to estimate the per capita killing efficacy one has to make assumptions on how the death rate of targets is functionally related to the number of epitope-specific T cells. This is generally unknown, and assuming different types of killing terms may change the estimated per capita killing efficacy by orders of magnitude. For example, at the peak of the CD8 T cell response to LCMV, there are $E \approx 1.1 \times 10^7$ NP396-specific CD8 T cells in the mouse spleen (6, 31). Assuming the mass-action killing term $K = kE$, the per capita killing efficacy of NP396-specific CD8 T cells is $k = K^a_{NP}/E \approx 4.5 \times 10^{-5}\ cell^{-1}\ day^{-1}$. However, if the death rate of pulsed targets were to saturate at high effector numbers, $K = kE/(1 + c_E E)$, then the estimated per capita killing rate depends on the half-saturation constant c_E, i.e., $k \approx c_E K$ (for $E \gg 1$). For $c_E = 10^{-6}$, one obtains $k \approx 5 \times 10^{-4}\ cell^{-1}\ day^{-1}$ which is 11 times higher than if the killing follows mass-action. Therefore, in the absence of solid knowledge of how to model target and CD8 T cell encounter in the spleen, estimating the death rate of pulsed targets due to CD8 T cell mediated killing seems to be most appropriate and robust.

Our analysis suggests that there is a correlation between the number of target cells entering the spleen from the blood at a given time point and the spleen size. Such a correlation may be expected to arise simply due to experimental techniques, since the total number of recruited cells in the spleen is calculated by multiplying the frequency of unpulsed targets in the spleen by the number of splenocytes. In the presence of measurement noise, this by itself leads to a positive correlation between spleen size and the number of cells, recruited to the spleen. Alternatively, a larger number of blood vessels in the spleen could lead both to a larger spleen

size and a larger cell entrapment area, and as the result, to a faster rate of recruitment of cells into a larger spleen. In this respect it is interesting to note that a two-fold slower rate of cell recruitment to the spleen in acutely infected as compared to memory mice (α_A vs. α_M, see Table 1) may indicate a decreased rate of cell immigration to the spleen from the circulation. This is likely to occur close to the peak of the immune response when many antigen-specific T cells leave lymphoid organs and migrate to peripheral tissues. Future studies need to address the migration pattern of splenocytes in mice and investigate potential mechanisms that may affect recruitment of target cells into the spleen.

We find that peptide-pulsed targets survive in acutely infected mice only for a few minutes. Such extremely short half-lifes are due to a large population of effector CD8 T cells present at the peak of the immune response. Because there are fewer memory CD8 T cells than effector CD8 T cells at the peak of the immune response, peptide-pulsed targets survive for longer times in LCMV-immune mice. Importantly, the overall killing efficacy of epitope-specific CD8 T cell response is correlated with the magnitude of the response. NP396-specific effectors reach the highest numbers at the peak of the response ($(1.1 \pm 0.6) \times 10^7$ per spleen), followed by GP276-specific effectors ($(3.6 \pm 1.4) \times 10^6$), NP396-specific memory CD8 T cells ($(3.3 \pm 2.5) \times 10^5$) and GP276-specific memory CD8 T cells ($(2.1 \pm 1.5) \times 10^5$). Therefore, a low killing efficacy of CD8 T cell responses observed in some studies could simply arise because of a small number of antigen-specific CD8 T cells and not because of a low per capita killing efficacy of CD8 T cells.

Comparing to previous studies (7, 37, 51), we provide the highest estimates for the death rate of peptide-pulsed targets in mice, acutely infected with LCMV, and in LCMV-immune mice. In their pioneering study, Barchet *et al.* (7) estimated the death rate of GP33-expressing targets to be about 5 per day. This is almost 100 fold lower than our estimate for the death rate of NP396-pulsed targets and about 14 times lower than the estimate for GP276-pulsed targets. This difference could arise due several reasons. First, Barchet *et al.* (7) assumed a rapid migration of target cells from the blood to the spleen. Assuming a similar rapid migration of cells into the spleen in our model led to dramatically lower estimates for the death rate of pulsed targets in acutely infected mice ($K^a_{NP} = 30\ day^{-1}$ and $K^a_{GP} = 16\ day^{-1}$ or about 5 to 15 times lower than the estimates given in Table 1). Second, Barchet *et al.* (7) used splenocytes from H8 mice that ubiquitously express the GP33 epitope of LCMV, and the level of expression of the endogenously produced peptide could be lower than that of a target cell pulsed with a high concentration of the specific peptide. Indeed, previous studies have found that the percent targets killed in the in vivo cytotoxicity assay depends on the amount of the peptide used for pulsing (6, 13). Finally, GP33-specific CD8 T cells may have a lower per capita killing efficacy than NP396- or GP276-specific CD8 T cells, leading also to the lower death rate of GP33-expressing targets.

Our estimates for the death rate of pulsed targets are also higher than those calculated

from a previous study by multiplying the estimated per capita killing efficacy of effector and memory CD8 T cells and their frequency in the mouse spleen (37). The main reason for this is that the model, proposed by the authors, poorly describes the early loss of NP396- and GP276-expressing targets in acutely infected mice (results not shown). We have shown that the early decline in the ratio of pulsed to unpulsed targets $R(t)$ is determined mainly by the death rate of pulsed targets due to CD8 T cell mediated killing. Therefore, a poor description of the early killing may lead to underestimation the killing efficacy of T cell responses. However, other reasons such as different fitting procedures employed in our and other studies may have contributed to different estimates of the death rate of targets (see, for example, (51)).

We find that NP396-expressing targets are killed by memory CD8 T cells at a rate 20 per day in the spleen (i.e., pulsed targets have a half-life of 48 minutes). Interestingly, since most of strains of LCMV replicate at rates less than 5-10 per day (10, 20), i.e., it takes 1 to 2 hours for a virus population to double its size, our estimates suggest that a NP396-specific memory CD8 T cell population can prevent virus regrowth in the spleen upon reinfection, and as such, could alone provide sterilizing immunity if memory cells were present at the right place and at the right time (cf., (17)).

Our analysis also allows one to calculate the number of target cells killed on average by one CD8 T cell per day (4, 48). This parameter is given simply by $KT(t)/E$ where K is the death rate of pulsed targets due to the CD8 T cell response, T is the number of targets expressing a particular epitope at time t after cell transfer, and E is the number of epitope-specific CD8 T cells in the spleen. Using the estimates for K from Table 1, we find that LCMV-specific memory CD8 T cells kill more target cells per day than effectors (Figure 4). This result may seem counter-intuitive since pulsed targets are eliminated much faster in acutely infected mice than in memory mice. However, acutely infected mice have 30 times more epitope-specific CD8 T cells, and because of that, on average, less than one target was killed by one effector CD8 T cell per day. In contrast, in some mice one memory CD8 T cell killed up to 20 targets per day.

Although this framework of estimation of death rates has been applied to measure killing in the spleen, it can be easily extended to measure killing in other organs of mice. If killing is measured for longer periods of time (say 12–24 hours), then the models analyzed here will have to be extended to allow 1) for recirculation of targets migrated to various organs, back to the blood, 2) potential changes in the number of epitope-specific CD8 T cells, and as the consequence, changes in the death rate of pulsed targets over time. Our report also emphasizes the importance of obtaining time series data on killing of peptide-pulsed targets because these allows for a more rigorous analysis of the data and also for testing of alternative models of killing. Application of this approach to measure killing efficacy of effector and memory CD8 T cell responses in other viral and bacterial infections will allow for more a quantitative understanding of immunology and potentially, may lead to better predictions of protective value of memory

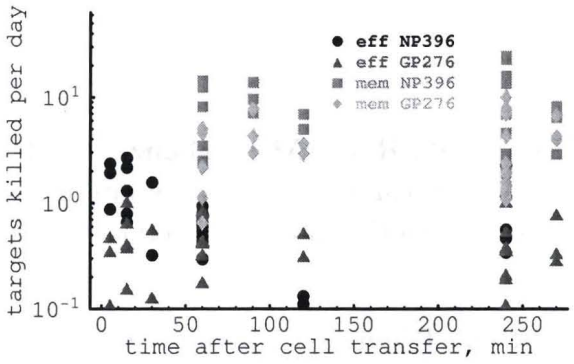

Figure 4: The average number of target cells killed per day by one epitope-specific effector or one memory CD8 T cell. The number of target cells killed per day is simply $KT(t)/E$ where $T(t)$ is the number of target cells taken from the data, K is the death rate of pulsed targets, and E is the average number of epitope-specific CD8 T cells in the spleen (see Table 1). Note that by calculating the average number of targets killed per day by one CD8 T cell we do not make any assumptions on the type of the killing term. Also note that the number of targets killed per day per CD8 T cell is not the per capita killing efficacy of CD8 T cells as it was estimated in previous studies (37, 51). The average number of target cells killed per day by a NP396-specific effector and memory CD8 T cell is 0.7 and 5.4, respectively, and for a GP276-specific effector and memory CD8 T cell is 1.2 and 4.2 cells per day, respectively.

CD8 T cells of different specificities.

Acknowledgments

We thank Joost Beltman, Kalet Leon, John Wherry, Dan Barber, Gennady Bocharov, Roland Regoes, Andrew Yates, and several referees for comments and suggestions during this work. This work was supported by the VICI grant 016.048.603 from NWO and a Marie Curie Incoming International Fellowship (FP6).

References

1. **Agnellini, P., Wolint, P., Rehr, M., Cahenzli, J., Karrer, U., and Oxenius, A.**, 2007. Impaired NFAT nuclear translocation results in split exhaustion of virus-specific CD8+ T cell functions during chronic viral infection. Proc Natl Acad Sci U S A **104**:4565–70.

2. **Aichele, P., Brduscha-Riem, K., Oehen, S., Odermatt, B., Zinkernagel, R., Hengartner, H., and Pircher, H.**, 1997. Peptide antigen treatment of naive and virus-immune mice: antigen-specific tolerance versus immunopathology. Immunity **6**:519–29.

3. **Antia, R., Ganusov, V., and Ahmed, R.**, 2005. The role of models in understanding CD8+ T-cell memory. Nat Rev Immunol **5**:101–111.

4. **Asquith, B., Mosley, A., Barfield, A., Marshall, S., Heaps, A., Goon, P., Hanon, E., Tanaka, Y., Taylor, G., and Bangham, C.**, 2005. A functional CD8+ cell assay reveals individual variation in CD8+ cell antiviral efficacy and explains differences in human T-lymphotropic virus type 1 proviral load. J Gen Virol **86**:1515–23.

5. **Assarsson, E., Sidney, J., Oseroff, C., Pasquetto, V., Bui, H. H., Frahm, N., Brander, C., Peters, B., Grey, H., and Sette, A.**, 2007. A quantitative analysis of the variables affecting the repertoire of T cell specificities recognized after vaccinia virus infection. J Immunol **178**:7890–901.

6. **Barber, D., Wherry, E., and Ahmed, R.**, 2003. Cutting edge: rapid in vivo killing by memory CD8 T cells. J Immunol **171**:27–31.

7. **Barchet, W., Oehen, S., Klenerman, P., Wodarz, D., Bocharov, G., Lloyd, A. L., Nowak, M. A., Hengartner, H., Zinkernagel, R. M., and Ehl, S.**, 2000.

Direct quantitation of rapid elimination of viral antigen-positive lymphocytes by antiviral CD8(+) T cells in vivo. Eur J Immunol **30**:1356–63.

8. **Bates, D. M. and Watts, D. G.**, 1988. Nonlinear regression analysis and its applications. John Wiles & Sons, Inc.

9. **Blattman, J. N., Antia, R., Sourdive, D. J., Wang, X., Kaech, S. M., Murali-Krishna, K., Altman, J. D., and Ahmed, R.**, 2002. Estimating the precursor frequency of naive antigen-specific CD8 T cells. J Exp Med **195**:657–6664.

10. **Bocharov, G., Ludewig, B., Bertoletti, A., Klenerman, P., Junt, T., Krebs, P., Luzyanina, T., Fraser, C., and Anderson, R.**, 2004. Underwhelming the immune response: effect of slow virus growth on CD8+-T-lymphocyte responses. J Virol **78**:2247–54.

11. **Brown, D., Dilzer, A., Meents, D., and Swain, S.**, 2006. CD4 T cell-mediated protection from lethal influenza: perforin and antibody-mediated mechanisms give a one-two punch. J Immunol **177**:2888–98.

12. **Busch, D. and Pamer, E.**, 1998. MHC class I/peptide stability: implications for immunodominance, in vitro proliferation, and diversity of responding CTL. J Immunol **160**:4441–8.

13. **Byers, A., Kemball, C., Moser, J., and Lukacher, A.**, 2003. Cutting edge: rapid in vivo CTL activity by polyoma virus-specific effector and memory CD8+ T cells. J Immunol **171**:17–21.

14. **Chiu, C., Heaps, A., Cerundolo, V., McMichael, A., Bangham, C., and Callan, M.**, 2007. Early acquisition of cytolytic function and transcriptional changes in a primary CD8+ T-cell response in vivo. Blood **109**:1086–1094.

15. **Coles, R., Mueller, S., Heath, W., Carbone, F., and Brooks, A.**, 2002. Progression of armed CTL from draining lymph node to spleen shortly after localized infection with herpes simplex virus 1. J Immunol **168**:834–8.

16. **Curtsinger, J., Lins, D., and Mescher, M.**, 2003. Signal 3 determines tolerance versus full activation of naive CD8 T cells: dissociating proliferation and development of effector function. J Exp Med **197**:1141–51.

17. **De Boer, R.**, 2007. Understanding the failure of CD8+ T-cell vaccination against simian/human immunodeficiency virus. J Virol **81**:2838–48.

18. **Doherty, P. C. and Christensen, J. P.**, 2000. Accessing complexity: the dynamics of virus-specific T cell responses. Annu Rev Immunol **18**:561–592.

19. **Efron, B. and Tibshirani, R.**, 1993. An introduction to the bootstrap. Chapman & Hall, New York.

20. **Ehl, S., Klenerman, P., Aichele, P., Hengartner, H., and Zinkernagel, R.**, 1997. A functional and kinetic comparison of antiviral effector and memory cytotoxic T lymphocyte populations in vivo and in vitro. Eur J Immunol **27**:3404–13.

21. **Filatenkov, A., Jacovetty, E., Fischer, U., Curtsinger, J., Mescher, M., and Ingulli, E.**, 2005. CD4 T cell-dependent conditioning of dendritic cells to produce IL-12 results in CD8-mediated graft rejection and avoidance of tolerance. J Immunol **174**:6909–17.

22. **Ford, W. and Simmonds, S.**, 1972. The tempo of lymphocyte recirculation from blood to lymph in the rat. Cell Tissue Kinet **5**:175–89.

23. **Fuller, M., Khanolkar, A., Tebo, A., and Zajac, A.**, 2004. Maintenance, loss, and resurgence of T cell responses during acute, protracted, and chronic viral infections. J Immunol **172**:4204–14.

24. **Ganusov, V. and De Boer, R.**, 2007. Do most lymphocytes in humans really reside in the gut? Trends Immunol **28**:514–8.

25. **Guarda, G., Hons, M., Soriano, S., Huang, A., Polley, R., Martin-Fontecha, A., Stein, J., Germain, R., Lanzavecchia, A., and Sallusto, F.**, 2007. L-selectin-negative CCR7- effector and memory CD8+ T cells enter reactive lymph nodes and kill dendritic cells. Nat Immunol **8**:743–52.

26. **Hataye, J., Moon, J., Khoruts, A., Reilly, C., and Jenkins, M.**, 2006. Naive and memory CD4+ T cell survival controlled by clonal abundance. Science **312**:114–6.

27. **Hawkins, E., Turner, M., Dowling, M., van Gend, C., and Hodgkin, P.**, 2007. A model of immune regulation as a consequence of randomized lymphocyte division and death times. Proc Natl Acad Sci U S A **104**:5032–5037.

28. **Hermans, I., Silk, J., Yang, J., Palmowski, M., Gileadi, U., McCarthy, C., Salio, M., Ronchese, F., and Cerundolo, V.**, 2004. The VITAL assay: a versatile fluorometric technique for assessing CTL- and NKT-mediated cytotoxicity against multiple targets in vitro and in vivo. J Immunol Methods **285**:25–40.

29. **Ingulli, E.**, 2007. Tracing Tolerance and Immunity In Vivo by CFSE-Labeling of Administered Cells. Methods Mol Biol **380**:365–76.

30. **Mueller, S., Jones, C., Smith, C., Heath, W., and Carbone, F.**, 2002. Rapid cytotoxic T lymphocyte activation occurs in the draining lymph nodes after cutaneous herpes simplex virus infection as a result of early antigen presentation and not the presence of virus. J Exp Med **195**:651–6.

31. **Murali-Krishna, K., Altman, J., Suresh, M., Sourdive, D., Zajac, A., Miller, J., Slansky, J., and Ahmed, R.**, 1998. Counting antigen-specific CD8+ T cells: A re-evaluation of bystander actiation during viral infection. Immunity **8**:177–187.

32. **Oehen, S. and Brduscha-Riem, K.**, 1998. Differentiation of naive CTL to effector and memory CTL: correlation of effector function with phenotype and cell division. J Immunol **161**:5338–46.

33. **Peixoto, A., Evaristo, C., Munitic, I., Monteiro, M., Charbit, A., Rocha, B., and Veiga-Fernandes, H.**, 2007. CD8 single-cell gene coexpression reveals three different effector types present at distinct phases of the immune response. J Exp Med **204**:1193–1205.

34. **Perelson, A. and Bell, G.**, 1982. Delivery of lethal hits by cytotoxic T lymphocytes in multicellular conjugates occurs sequentially but at random times. J Immunol **129**:2796–801.

35. **Perelson, A. and Macken, C.**, 1985. Quantitative models for the kinetics of cell-mediated cytotoxicity at the single cell level. Adv Exp Med Biol **184**:551–61.

36. **Perelson, A., Macken, C., Grimm, E., Roos, L., and Bonavida, B.**, 1984. Mechanism of cell-mediated cytotoxicity at the single cell level. VIII. Kinetics of lysis of target cells bound by more than one cytotoxic T lymphocyte. J Immunol **132**:2190–8.

37. **Regoes, R., Barber, D., Ahmed, R., and Antia, R.**, 2007. Estimation of the rate of killing by cytotoxic T lymphocytes in vivo. Proc Natl Acad Sci U S A **104**:1599–603.

38. **Reynolds, J., Heron, I., Dudler, L., and Trnka, Z.**, 1982. T-cell recirculation in the sheep: migratory properties of cells from lymph nodes. Immunology **47**:415–21.

39. **Smith, M. and Ford, W.**, 1983. The recirculating lymphocyte pool of the rat: a systematic description of the migratory behaviour of recirculating lymphocytes. Immunology **49**:83–94.

40. **Stambas, J., Doherty, P., and Turner, S.**, 2007. An in vivo cytotoxicity threshold for influenza A virus-specific effector and memory CD8(+) T cells. J Immunol **178**:1285–92.

41. **Tian, S., Maile, R., Collins, E., and Frelinger, J.**, 2007. CD8+ T cell activation is governed by TCR-peptide/MHC affinity, not dissociation rate. J Immunol **179**:2952–60.

42. **Tzelepis, F., Persechini, P., and Rodrigues, M.**, 2007. Modulation of CD4+ T cell-dependent specific cytotoxic CD8+ T cells differentiation and proliferation by the timing of increase in the pathogen load. PLoS ONE **2**:e393.

43. **van der Burg, S. H., Visseren, M. J., Brandt, R. M., Kast, W. M., and Melief, C. J.**, 1996. Immunogenicity of peptides bound to MHC class I molecules depends on the MHC-peptide complex stability. J Immunol **156**:3308–14.

44. **van Stipdonk, M., Hardenberg, G., Bijker, M., Lemmens, E., Droin, N., Green, D., and Schoenberger, S.**, 2003. Dynamic programming of CD8+ T lymphocyte responses. Nat Immunol **4**:361–5.

45. **Westermann, J., Ehlers, E., Exton, M., Kaiser, M., and Bode, U.**, 2001. Migration of naive, effector and memory T cells: implications for the regulation of immune responses. Immunol Rev **184**:20–37.

46. **Westermann, J., Persin, S., Matyas, J., van der Meide, P., and Pabst, R.**, 1994. Migration of so-called naive and memory T lymphocytes from blood to lymph in the rat. The influence of IFN-gamma on the circulation pattern. J Immunol **152**:1744–50.

47. **Westermann, J., Sollner, S., Ehlers, E., Nohroudi, K., Blessenohl, M., and Kalies, K.**, 2003. Analyzing the migration of labeled T cells in vivo: an essential approach with challenging features. Lab Invest **83**:459–69.

48. **Wick, W., Yang, O., Corey, L., and Self, S.**, 2005. How many human immunodeficiency virus type 1-infected target cells can a cytotoxic T-lymphocyte kill? J Virol **79**:13579–86.

49. **Wolint, P., Betts, M., Koup, R., and Oxenius, A.**, 2004. Immediate cytotoxicity but not degranulation distinguishes effector and memory subsets of CD8+ T cells. J Exp Med **199**:925–36.

50. **Yarke, C., Dalheimer, S., Zhang, N., Catron, D., Jenkins, M., and Mueller, D.**, 2008. Proliferating CD4+ T Cells Undergo Immediate Growth Arrest upon Cessation of TCR Signaling In Vivo. J Immunol **180**:156–62.

51. **Yates, A., Graw, F., Barber, D. L., Ahmed, R., Regoes, R. R., and Antia, R.**, 2007. Revisiting Estimates of CTL Killing Rates In Vivo. PLoS ONE **2**:e1301.

52. **Yewdell, J.**, 2006. Confronting complexity: real-world immunodominance in antiviral CD8+ T cell responses. Immunity **25**:533–43.

53. **Zar, J.**, 1999. Biostatistical Analysis. Prentice Hall, Upper Saddle River, NJ.